

Chapter 16

Primary Standards for Brachytherapy Sources

Michael G. Mitch, Ph.D., and Christopher G. Soares, Ph.D.
Physics Laboratory, National Institute of Standards and Technology
Gaithersburg, Maryland

1. Low-Energy Low Dose-Rate (LDR) Brachytherapy Seeds	549
1.1 Introduction	549
1.2 NIST Air-Kerma Strength Standard	550
1.3 Other Primary Air-Kerma-Rate Measurements	552
2. High-Energy LDR Brachytherapy Sources	553
2.1 Introduction	553
2.2 NIST Air-Kerma-Strength Standard	553
2.3 NPL Air-Kerma-Rate Standard for LDR ¹⁹² Ir Sources	554
3. High-Energy High Dose-Rate (HDR) Brachytherapy Sources	555
3.1 Introduction	555
3.2 Interpolation Technique for ¹⁹² Ir and ¹⁶⁹ Yb Sources	555
3.3 Direct Methods for Air-Kerma-Rate and Absorbed-Dose-Rate Measurements	557
4. Beta-Particle-Emitting Brachytherapy Sources	557
4.1 Introduction	557
4.2 NIST Medical Extrapolation Chamber	558
4.3 Other Primary Standard Extrapolation Chambers	559
5. Secondary Standards for Clinical Brachytherapy Source Measurements	560
5.1 Introduction	560
5.2 Well-Ionization Chambers	560
5.3 Detectors for Absorbed-Dose Measurements	562
References	563
Problems	565

1. Low-Energy Low Dose-Rate (LDR) Brachytherapy Seeds

1.1 Introduction

The American Association of Physicists in Medicine (AAPM) dosimetry protocol for low dose-rate (LDR) brachytherapy seeds that emit x-rays of energies ≤ 50 keV is described in the updated Task Group 43 report (TG-43U1) (Rivard et al. 2004). In this protocol, it is specified that the strength of such sources be expressed in

terms of air-kerma strength, traceable to the National Institute of Standards and Technology (NIST). NIST maintains and disseminates a primary air-kerma-strength standard for all ^{125}I , ^{103}Pd , and ^{131}Cs seed models.

1.2 NIST Air-Kerma Strength Standard

At NIST, the quantity air kerma is directly realized using the Wide-Angle Free-Air Chamber (WAFAC), a cylindrically symmetric free-air ionization chamber, shown schematically in figure 16-1 (Seltzer et al. 2003). The WAFAC differs from a “traditional” free-air chamber, such as that used to realize air kerma from x-ray beams (see chapter 15), in that the x-rays emergent from the brachytherapy source do not travel through the air volume of the chamber unperturbed by materials of the chamber itself. The much weaker intensity of seed emissions necessitates the use of a large (8 cm) diameter aperture as opposed to, for example, a 1 cm aperture for beam measurements. As a result, the photons from the seeds actually pass through the high-voltage and collection electrodes, which are made of thin, aluminized polyethylene terephthalate (PET). To account for any perturbations due to secondary electrons originating in the electrodes, ionization current measurements are performed at two volumes and the net current and volume are used in the calculation of air kerma. The air-kerma rate, $\dot{K}_{air}(Q)$, is determined using the equation

$$\dot{K}_{air}(Q) = \left(\frac{\bar{W}}{e} \right) \left(\frac{1}{\rho_{air} V_{eff}} \right) K_{dr}(\dot{K}) M_{det}(\dot{K}, Q) \prod_i K_i \prod_j K_j(Q), \quad (16.1)$$

where \bar{W} is the mean energy per ion pair expended when the initial kinetic energy of a charged particle is completely dissipated in air, e is the elementary charge, ρ_{air} is the density of air, V_{eff} is the product of the area of the aperture and the length difference between the two collection volumes, $K_{dr}(\dot{K})$ is the recombination correction, $M_{det}(\dot{K}, Q)$ is the difference in current measured for the two collection volumes (corrected for radioactive decay), K_i are correction factors that are independent of the spectrum, and K_j are correction factors that are spectrum dependent (see table 16-1). The air-kerma strength, S_K , is calculated from $\dot{K}_{air}(Q)$ by the equation

$$S_K = \dot{K}_{air}(Q) d^2, \quad (16.2)$$

where d is the distance between the source and the back plane of the aperture (nominally 30 cm). According to TG-43U1, the air-kerma strength should not include contributions from photons of energy <5 keV, because such low-energy x-rays do not significantly contribute to the dose in tissue at distances greater than 1 mm (Taylor and Rogers 2008). Many seed models use titanium as the encapsulation material, which results in 4.5 keV fluorescence photons being part of the emergent spectrum. An aluminum filter of thickness 0.08636 mm is interposed between

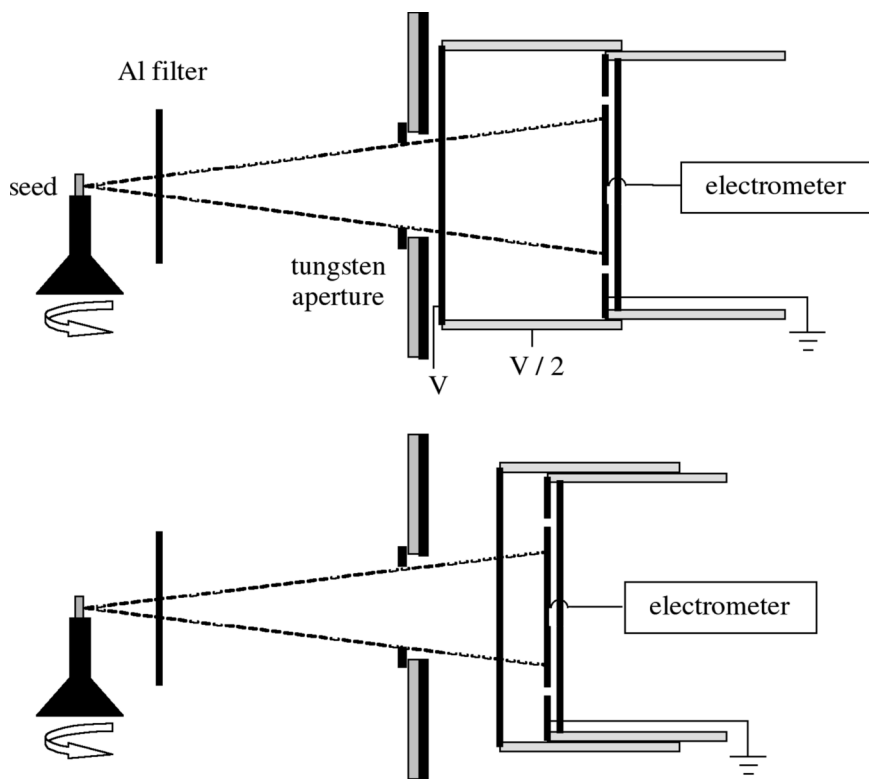


Figure 16-1. Schematic diagram of the WAFAC (not to scale), showing the electrode positions for the large (top) and small (bottom) collection volumes. Note that the distance between the seed and the center of the chamber volume remains constant.

the source and the WAFAC entrance aperture to remove these photons from the seed spectrum. As the air-kerma strength is specified *in vacuo*, appropriate corrections for air (and filter) attenuation and scattering are applied to the measurements (see table 16-1). The seed is mounted vertically and rotated at one revolution per minute around its long axis during measurements to average over any equatorial anisotropy in the emergent photon fluence. Such anisotropy is characterized by performing ionization current measurements at discrete 45-degree rotation increments with the WAFAC in the large volume configuration. The response of the WAFAC to a ^{241}Am source (emissions include 60 keV photons) is periodically measured to verify the continued stability of the system.

It is worth mentioning that air-kerma strength, as calculated from the air-kerma rate, implies that the inverse-square law holds true, and that the seed and WAFAC

Table 16-1: Correction Factors for WAFAC Measurement of ^{125}I and ^{103}Pd Brachytherapy Sources (Seltzer et al. 2003)

	^{125}I	^{103}Pd
Decay correction, K_1	$T_{1/2} = 59.43 \text{ d}$	$T_{1/2} = 16.991 \text{ d}$
Recombination, $K_{dr}(\dot{K})$	<1.004	<1.004
Attenuation in filter, $K_3(Q)$	1.0295	1.0738
Air attenuation in WAFAC, $K_4(Q)$	1.0042	1.0079
Source-aperture attenuation, $K_5(Q)$	1.0125	1.0240
Inverse-square correction, K_6	1.0089	1.0089
Humidity, $K_7(Q)$	0.9982	0.9981
In-chamber photon scatter, $K_8(Q)$	0.9966	0.9962
Source-holder scatter, K_9	0.9985	0.9985
Electron loss, K_{10}	1.0	1.0
Aperture penetration, $K_{11}(Q)$	0.9999	0.9999
External photon scatter, $K_{12}(Q)$	1.0	1.0

approximate a point source and detector, respectively, at the calibration distance of 30 cm. It has been shown that depending on the geometry and materials used in seed construction, significant deviations from the inverse square law are possible due to source self-attenuation and scattering effects (Monroe and Williamson 2002). Also, the large collecting volume of the WAFAC does not approximate a point detector. However, any practical ionization chamber will necessarily include deviations from the ideal, nonexistent “zero volume” detector. Therefore, the averaging over the conical beam (7.6-degree half-angle) must be accepted as being an inherent part of this instrument-based primary standard.

1.3 Other Primary Air-Kerma-Rate Measurements

There are several laboratories other than NIST that have developed methods of measuring the air-kerma rate of LDR brachytherapy seeds. The Physikalisch-Technische Bundesanstalt (PTB) built a parallel plate extrapolation chamber with cylindrical geometry and a large volume called the Grossvolumen Extrapolationskammer (GROVEX) (Selbach et al. 2008). The Variable-Aperture Free-Air Chamber (VAFAC) was developed at the University of Wisconsin (Culbertson et al. 2006). The VAFAC is similar in design to the WAFAC, except that it has a larger volume and is able to measure the air-kerma strength of sources greater than 1 cm in length by employing a series of apertures with diameters from 5.0 cm to 16.5 cm. Both the GROVEX and the VAFAC are

operated as extrapolation chambers, which are parallel-plate ionization chambers whose volumes are continuously variable. For these chambers, the slope of the ionization current versus plate separation curve is used to calculate the air-kerma rate, $\dot{K}_{air}(Q)$, using the equation

$$\dot{K}_{air}(Q) = \left(\frac{\bar{W}}{e}\right) \left(\frac{1}{\rho_{air} A_{eff}}\right) \left(\frac{dM_{det}(\dot{K}, Q)}{ds}\right) \prod_i K_i(\dot{K}, Q), \quad (16.3)$$

where A_{eff} is the effective area of the collection electrode, s is the plate separation distance; other quantities have been defined previously.

The National Physical Laboratory (NPL) calibrates ^{125}I seeds in terms of air-kerma rate with a well-type ionization chamber, having a calibration traceable to the NPL air-kerma primary standard for low-energy x-rays (Baker et al. 2002). Air-kerma is realized by a 3 L spherical ionization chamber with a thin, graphite-coated carbon fiber wall positioned at a distance of 1 m from the source. The calibration coefficient for ^{125}I seeds is derived from an average of coefficients for 25 keV and 33 keV ISO 4037 Narrow Spectrum x-ray beams. The Laboratoire National Henri Becquerel (LNHB) has built a unique torus-shaped free-air chamber, which eliminates the need to rotate the seed during measurements and subtends a smaller angle near the axis of the seed (Soares et al. 2009).

2. High-Energy LDR Brachytherapy Sources

2.1 Introduction

For LDR brachytherapy sources that emit photons with average energy >50 keV, the AAPM and the European Society for Therapeutic Radiology and Oncology (ESTRO) have issued joint recommendations for the dosimetry of such sources (Li et al. 2007). The air-kerma strength of sources containing either the radionuclide ^{192}Ir or ^{137}Cs must be traceable to the appropriate primary standard.

2.2 NIST Air-Kerma-Strength Standard

The air-kerma rate of ^{192}Ir and ^{137}Cs brachytherapy sources is directly realized at NIST using a variety of spherical, graphite-walled cavity ionization chambers (Seltzer and Bergstrom 2003). Measurements are performed free-in-air at source-to-chamber distances between 0.5 m and 1.0 m with a chamber of volume and wall thickness such that Bragg-Gray conditions are satisfied. The air-kerma rate, $\dot{K}_{air}(Q)$, is calculated using the equation

$$\dot{K}_{air}(Q) = \left(\frac{\bar{W}}{e}\right) \left(\frac{1}{\rho_{air} V}\right) \left(\frac{1}{1-\bar{g}}\right) \frac{(\bar{\mu}_{en} / \rho)_{air} (\bar{L}_{\Delta} / \rho)_{gr}}{(\bar{\mu}_{en} / \rho)_{gr} (\bar{L}_{\Delta} / \rho)_{air}} K_{dr}(\dot{K}) M_{det}(\dot{K}, Q) K_{stem} K_{wall}(Q) K_h(Q), \quad (16.4)$$

where

\bar{W} , e , and ρ_{air} were defined previously,

V is the volume of air in the chamber,

\bar{g} is the mean fraction of kinetic energy lost by charged particles in radiative processes,

$\bar{\mu}_{en} / \rho$ is the mean photon-energy-fluence-weighted mass energy-absorption coefficient,

\bar{L}_{Δ} / ρ is the mean Spencer-Attix electron-fluence-weighted electron mass stopping power,

$K_{dr}(\dot{K})$ is the recombination correction,

$M_{det}(\dot{K}, Q)$ is the net current (corrected for radioactive decay),

K_{stem} is the stem-scatter correction factor,

$K_{wall}(Q)$ is the wall correction factor, and

$K_h(Q)$ is the humidity correction factor.

The air-kerma strength is calculated from $\dot{K}_{air}(Q)$ as shown in equation (16.2).

The graphite cavity chamber for ^{137}Cs source calibrations has a volume of about 1 cm^3 , and was used to calibrate several “working standard” sources (Loftus 1969). These same sources are used to determine the air-kerma strength of unknown sources through a replacement method. The ionization current from an aluminum, 2.8 L spherical cavity chamber is measured for both the working standard and the unknown source. The air-kerma strength for the unknown source is then obtained by multiplying the air-kerma strength of the working standard source by the ratio of the ionization current due to the unknown source to that of the working standard source. LDR ^{192}Ir sources were calibrated using a graphite cavity chamber with a volume of 50 cm^3 (Loftus 1979). Despite using a larger-volume chamber, the relatively weak intensity of ^{192}Ir seeds compared to that of ^{137}Cs sources required that an array of about 50 seeds be used for the measurement. To determine the air-kerma strength of individual ^{192}Ir seeds, the calibration coefficient of a 3.4 L aluminum re-entrant chamber was calculated as the quotient of the air-kerma strength of the 50-seed array and the sum of the individual re-entrant chamber currents for all 50 seeds. Each calibration of an ^{192}Ir seed performed with the re-entrant chamber is accompanied by a measurement of ionization current from a ^{226}Ra source (with a half-life of 1600 years) to verify the consistency of the re-entrant chamber response over time.

2.3 NPL Air-Kerma-Rate Standard for LDR ^{192}Ir Sources

NPL measures the air-kerma rate from ^{192}Ir wires and pins in an open-air geometry with a thin-walled spherical cavity chamber, described previously in section 1.3 (Rossiter et al. 1991). The calibration coefficient of the chamber is determined based on the known photon energy spectrum emerging from the ^{192}Ir sources and its known response to beams of x-rays (33 keV to 250 keV), ^{137}Cs , and ^{60}Co . The calibration is also transferred to a well-ionization chamber (Sephton et al. 1993).

3. High-Energy High Dose-Rate (HDR) Brachytherapy Sources

3.1 Introduction

Guidelines from the AAPM and ESTRO for the dosimetry of high-energy, high dose-rate (HDR) and pulsed dose-rate (PDR) brachytherapy sources have recently been published (Li et al. 2007). Since no NIST air-kerma-strength standard presently exists for HDR ^{192}Ir and ^{169}Yb sources, use of the secondary standard for such sources currently maintained by the AAPM Accredited Dosimetry Calibration Laboratories (ADCLs) is recommended. Several national standards laboratories outside the United States currently maintain a primary standard for HDR ^{192}Ir sources, including the NPL, LNHB, PTB, Nederlands Meetinstituut (NMI), and Bhabha Atomic Research Centre (BARC).

3.2 Interpolation Technique for ^{192}Ir and ^{169}Yb Sources

The air-kerma-strength standard for HDR ^{192}Ir sources as maintained by the ADCLs uses the “seven distance” technique employing a 3.6 cm^3 spherical cavity ionization chamber with an air-equivalent plastic wall (Goetsch et al. 1991). NIST traceability is achieved in the calibration coefficient for the ionization chamber by linear interpolation between the calibration coefficients for the NIST ^{137}Cs and M250 x-ray beam air-kerma primary standards. This method yields satisfactory results since the average gamma-ray energy for ^{192}Ir is about midway between that of ^{137}Cs and M250 x-rays, and the chamber response is reasonably flat over the range of energies involved. The air-kerma calibration coefficient for the chamber, N_K^{lr} is calculated using the formula

$$N_K^{lr} = \frac{K_{wall}^{M250}(Q)N_K^{M250} + K_{wall}^{Cs}(Q)N_K^{Cs}}{2K_{wall}^{lr}(Q)}, \quad (16.5)$$

where $K_{wall}^{M250}(Q)$, $K_{wall}^{Cs}(Q)$, and $K_{wall}^{lr}(Q)$ are the chamber wall corrections for the M250 beam, ^{137}Cs , and ^{192}Ir , respectively. N_K^{M250} and N_K^{Cs} are the chamber calibration coefficients (air-kerma rate per unit current) obtained from NIST. The result of ionization current measurements at each of seven source-to-chamber distances, $M_{det}(\dot{K}, Q)$, is composed of contributions from both the primary radiation and the scattered radiation, M_{scat} . To obtain air-kerma rate, $\dot{K}_{air}(Q)$, only the contribution from the primary radiation is included, such that

$$\dot{K}_{air}(Q) = N_K^{lr} [M_{det}(\dot{K}, Q) - M_{scat}] \quad (16.6)$$

and the air-kerma strength, S_K , is calculated using the equation

$$S_K = \dot{K}_{air}(Q)(d+c)^2, \quad (16.7)$$

where d is the source-to-chamber distance and c accounts for any offset in the distance measurement. The three unknowns in equations (16.6) and (16.7), namely S_K , M_{scat} , and c , may be found by solving the set of simultaneous equations resulting from measurements at multiple distances.

An alternative method for calculating N_K^{lr} has been proposed which states that the chamber response coefficient, $(N_K^{lr})^{-1}$, should be determined by calculating the air-kerma-weighted average of $(N_K^{Ei})^{-1}$ over the lines of energy Ei in the ^{192}Ir source spectrum (Mainegra-Hing and Rogers 2006):

$$\frac{1}{N_K^{lr}} = \sum_i \frac{K_{air}^{Ei}}{K_{air}^{lr}} \left(\frac{1}{N_K^{Ei}} \right), \quad (16.8)$$

where K_{air}^{Ei} and K_{air}^{lr} are the air-kerma contribution from spectrum line of energy Ei and the total air kerma, respectively. Approximating the spectrum of ^{192}Ir as M250 x-ray and ^{137}Cs gamma-ray beams of equal air-kerma rates yields

$$\frac{1}{N_K^{lr}} = \frac{\left(\frac{1}{N_K^{M250}} + \frac{1}{N_K^{Cs}} \right)}{2}. \quad (16.9)$$

Note that in contrast to equation (16.5), this method does not require knowledge of the chamber wall correction factors.

Other national standards laboratories offer calibrations of HDR and PDR ^{192}Ir brachytherapy sources using a variety of methods. At LNHB the method of Goetsch is used, with the ionization chamber rotated in the transverse plane about the source to minimize errors in source to chamber distance measurements (Douysset et al. 2005). The PTB uses a robotic system for precise positioning of the chamber in the radiation beam, and the source is placed in a lead housing with a collimator to reduce the contribution of scattered radiation to the chamber signal. A shield in the shape of a cone, designed to match the beam profile, can be inserted between the source and the chamber, thus blocking the direct beam and allowing the ionization current due only to scattering to be measured. The NMI determines the calibration coefficient for its ionization chamber using eight photon beams ranging in energy from 48 keV to 1250 keV, then calculates N_K^{lr} by weighting the individual N_K^{Ei} values for each beam by the ^{192}Ir spectrum peak heights (van Dijk et al. 2004).

The Goetsch seven-distance method has also been applied to measure the air-kerma rate of HDR ^{169}Yb brachytherapy sources (Das et al. 1995; VanDamme et al. 2008). In the work of Das et al., a 100 cm³ spherical cavity ionization chamber with air-equivalent plastic walls was used for the measurement. The calibration coefficient for the chamber, N_K^{Yb} , was calculated based on a piecewise linear fit of NIST-

traceable calibration coefficients for ^{137}Cs gamma rays and four x-ray beams of effective energies from about 50 keV to 150 keV, namely the NIST heavily filtered x-ray beams H60, H100, H200, and H300. In the study by VanDamme et al., the calibration coefficient of the 30 cm³ ionization chamber was determined as a function of energy by performing a least-squares fit of the response coefficients, $(N_{Kj}^{Yb})^{-1}$ for each of the i lines in the ^{169}Yb spectrum, weighting each coefficient by the fractional line intensity, W_i :

$$N_K^{Yb} = \left[\sum_i W_i (N_{Kj}^{Yb})^{-1} \right]^{-1}. \quad (16.10)$$

The N_{Kj}^{Yb} values were derived from chamber calibration coefficients.

3.3 Direct Methods for Air-Kerma-Rate and Absorbed-Dose-Rate Measurements

Directly realizing the air-kerma rate from an HDR ^{192}Ir source requires that ionization chamber correction factors be determined explicitly from the ^{192}Ir spectrum emergent from the source, as opposed to using an interpolation method as described in section 3.2. Since the energies of photons emitted during the decay of ^{192}Ir are too low for Bragg-Gray theory to be applied, Monte Carlo methods have been used to calculate chamber correction factors (Borg et al. 2000). NPL uses a spherical graphite ionization chamber with a collimated beam geometry to perform HDR ^{192}Ir source calibrations (Sander and Nutbrown 2006).

An alternative approach to an air-kerma-rate standard is the concept of an absorbed-dose-to-water standard for HDR ^{192}Ir sources using water calorimetry (Sarfehnia et al. 2007). Although the uncertainty of such a measurement is expected to be larger than that of an air-kerma-rate measurement, estimated to be about 5% versus 1%, the water calorimeter directly realizes the quantity of interest in medical dosimetry of absorbed dose to water (tissue). As this calorimeter method is refined, it is expected that uncertainties will decrease, and the need to convert an air-kerma rate to absorbed dose using a dose rate constant may be eliminated.

4. Beta-Particle-Emitting Brachytherapy Sources

4.1 Introduction

Unlike the photon brachytherapy source standards described above, beta particle brachytherapy standards realize the quantity absorbed dose to water or tissue. All primary standards for beta particle source dosimetry are based upon extrapolation ionization chambers. The Bragg-Gray principle is used to convert ionization

density (current per unit air volume) to absorbed dose rate to water, $\dot{D}_w(Q)$, according to the equation

$$\dot{D}_w(Q) = \left(\frac{\bar{W}}{e} \right) \left(\frac{1}{\rho_{air} A_{eff}} \right) S_{w,a}(Q) \left[\frac{d}{d\ell} \Pi k' M_{det}(\ell) \right]_{\ell=0} \Pi k, \quad (16.11)$$

where \bar{W}/e , ρ_{air} , and A_{eff} are defined previously; and $S_{w,a}(Q)$ is the ratio of the mean mass-collision stopping powers in water to air for beta particle radiation of quality Q , Πk is the product of the correction factors which are independent of the chamber depth, $\left[\frac{d}{d\ell} \Pi k' M_{det}(\ell) \right]_{\ell=0}$ is the limiting value of the slope of the corrected

current $M_{det}(\ell)$ versus chamber depth, ℓ , function, and $\Pi k'$ is the product of the correction factors which vary with the chamber depth. The Bragg-Gray stopping power ratio $S_{w,a}(Q)$ is given by

$$S_{w,a}(Q) = \frac{\int_0^{E_{max}} (\Phi_E)_w (S/\rho)_{col,w} dE}{\int_0^{E_{max}} (\Phi_E)_w (S/\rho)_{col,a} dE} \quad (16.12)$$

where $(\Phi_E)_w$ is the spectrum of electrons at the reference point of the extrapolation chamber, $(S/\rho)_{col,w}$ is the mass-collision stopping power for an electron with kinetic energy E in water and $(S/\rho)_{col,a}$ is the corresponding quantity for air. It is assumed that secondary electrons (delta rays) deposit their energy where they are generated or are in complete CPE (charged particle equilibrium) so that they are not included in the electron fluence. The upper limit of the integrals is given by the maximum energy, E_{max} , of the beta radiation in the fluence spectrum and the lower limit corresponds to the lowest energy in the spectrum, here indicated by a zero. In principle, this spectrum also includes any electrons set in motion by bremsstrahlung photons, but these are usually of negligible importance.

Examples of corrections that are independent of chamber depth include a correction for the difference in backscatter between the collecting electrode material and water, and a correction for attenuation of beta particles in the entrance window of the extrapolation chamber. Corrections that are dependent on chamber depth include corrections for variations in ambient temperature and pressure to reference conditions, recombination, and the effect of beam divergence and walls.

4.2 NIST Medical Extrapolation Chamber

The extrapolation chamber used at NIST as a primary standard for beta particle sources used for medical applications is based on a design by Loevinger (Loevinger and Trott 1966). At the measurement distances employed for medical beta particle sources (contact to a few millimeters in water-equivalent materials)

the main feature of the corrected current versus electrode separation function is a sublinearity at larger electrode separations, which occurs due to the effect of the extreme source-field divergence near the source surface. To minimize this effect, measurements are performed at electrode separations as small as possible, usually between about 50 μm and 150 μm , and Monte Carlo-based divergence corrections are applied.

For the measurement of planar beta particle sources at the source surface or at depth in water-equivalent material, a collecting electrode with a 4 mm diameter is used (Soares 1991). To properly position this electrode at the source center, a mapping of the dose-rate distribution at the source surface is first performed using a collecting electrode with a 1 mm diameter. To do this, an automated two-dimensional positioning system is employed. From this distribution, the source center is determined, the source is centered with the collecting electrode axis, the 1 mm diameter electrode is replaced with the 4 mm diameter electrode, and the extrapolation measurement is performed.

For beta-particle seed and line sources, the 1 mm electrode is used to measure absorbed dose rate at the surface of tissue-equivalent phantoms in which the sources are placed (Soares et al. 1998). Although a range of phantom blocks have been made over the years, most often the sources are measured at the reference depth of 2 mm. As with the planar sources, the dose distribution on the block surface is first mapped with the 1 mm collecting electrode to determine the central point of the dose distribution where the extrapolation measurement will take place.

4.3 Other Primary Standard Extrapolation Chambers

The primary standard of PTB is a novel extrapolation chamber based on a newly designed multi-electrode extrapolation chamber (MEC) that meets the requirements of high spatial resolution and small uncertainty in measurement (Bambynek 2002). In contrast to a conventional extrapolation chamber, the central part of the MEC is a segmented collecting electrode fabricated using electron beam lithography on an alumina or silicon wafer. A large number (30 or more) of collecting electrodes 1 mm by 1 mm in size are arranged in the center of the wafer. A precise displacement device consisting of three piezoelectric macro-translators changes the chamber depth by moving the wafer collecting electrode relative to the fixed entrance window. Use of this chamber allows a simultaneous mapping of the absorbed dose distribution as well as the determination of reference absorbed dose rate.

The beta radiation source standard extrapolation chamber of the NMI is of a design similar to the NIST extrapolation chamber. As in the NIST chamber, the collecting electrode remains stationary while the entrance window is moved to change the collecting volume, and a precision three-dimensional stage moves the source to allow centering, field mapping, and maintenance of the position relative to the entrance electrode as the volume is changed. The collecting electrode is 1 mm in diameter, and is constructed from D400 water-equivalent plastic.

5. Secondary Standards for Clinical Brachytherapy Source Measurements

5.1 Introduction

Once a primary air-kerma strength or absorbed dose standard has been realized by a national standards laboratory, a method of accurately transferring that standard to secondary calibration laboratories and therapy clinics must be developed. Since absolute accuracy is not required, a simple measurement method of high precision is desired. In the case of both photon- and beta-emitting brachytherapy sources, well-ionization chambers provide an effective means of accomplishing such a transfer. For beta sources, where source non-uniformity could significantly impact well chamber response, imaging the distribution of radioactive material within the source using radiochromic film is also employed.

5.2 Well-Ionization Chambers

5.2.1 X-Ray and Gamma Sources

As the name implies, well-ionization chambers are cylindrical in shape with a well located along the central axis where a radioactive source is placed. Photons from the source ionize the counting gas, which may be air or another gas, such as argon. The liberated charge (or ionization current) is measured with an electrometer, and if the chamber is open to the atmosphere, corrected to conditions of standard temperature and pressure (22 °C and 760 mmHg) and for radioactive decay to a given reference time and date. When measuring the response of a well chamber to a brachytherapy source, it is very important to be able to reproducibly position the source in the well. A centering jig with a thin-walled tube is typically used, capable of holding the source at the position of maximum response, or “sweet spot.” It is good practice to verify that the chamber’s response remains constant over time by periodically measuring a check source containing a long-lived radionuclide and plotting the results on a control chart.

A well chamber is calibrated by measuring its response to a source that has been calibrated by a primary standards laboratory in terms of air-kerma strength, S_K . The calibration coefficient, S_K/I , is defined as the ratio of the air-kerma strength to the well chamber ionization current, I , typically expressed in units of U/A, where $1 \text{ U} = 1 \mu\text{Gy m}^2/\text{h}$. Traceability to the primary S_K standard for a given source model thus resides in the well chamber calibration coefficient. Such a calibrated instrument is used by secondary standards laboratories to maintain their in-house standard. Measuring the well chamber current for an unknown source and multiplying by the calibration coefficient yields an air-kerma strength value that is traceable to national standards. It must be emphasized that a given calibration coefficient is only valid for the particular source model used to calibrate the well chamber. Secondary standards laboratories calibrate well chambers for clinics by first cali-

brating a source in terms of air-kerma strength with their in-house standard, then using that same source to measure the response (I) of, and calculate the calibration coefficient (S_K/I) for, the clinical chamber. Medical physicists may then use their calibrated well chamber to measure the S_K value for sources as a quality assurance check prior to use.

For high-energy gamma-emitting brachytherapy sources, such as those containing ^{137}Cs , the value of the calibration coefficient is relatively insensitive to small changes in source encapsulation geometry (cylinders versus needles) due to the negligible attenuation of the gamma rays by the capsule for such energies. However, for low-energy x-ray emitting ^{125}I , ^{103}Pd , and ^{131}Cs brachytherapy sources, minor changes in source construction may have a significant effect on the calibration coefficient. This is due to the fact that the wall of the well between the source and the counting gas, particularly on chambers filled with pressurized gas that require a thick wall, could strongly attenuate the low-energy photons, causing the response curve to change rapidly as a function of energy. This effect is observed in the case of ^{125}I sources, where models which contain silver as part of the internal construction will have fluorescence x-rays from the silver in the emergent spectrum in addition to photons from the ^{125}I decay. Since the silver x-rays are lower in energy than those from ^{125}I , the average energy of the spectrum will be lower, along with the response of the well chamber relative to the air-kerma strength as realized by a free-air chamber. The result is that calibration coefficients for ^{125}I sources that contain silver are about 10% higher than those for sources with no silver (see figure 16-2).

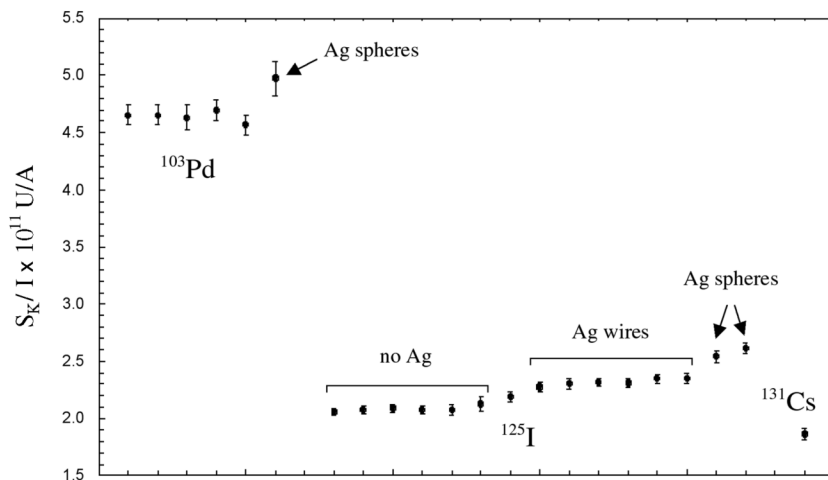


Figure 16-2. Well chamber calibration coefficients (air-kerma strength per unit current) for 6 models of ^{103}Pd , 15 models of ^{125}I , and 1 model of ^{131}Cs brachytherapy seeds.

In addition to changes in the emergent spectrum, differences in the anisotropy of emissions around the source may also influence well chamber calibration coefficients (Mitch et al. 2002). Because of the difference in the measurement geometry between primary air-kerma strength standards, typically a conical beam defined by the aperture on a free-air chamber or intercepted by the cross section of a cavity chamber, and well chambers, which detect radiation in almost a 4π solid angle, even source models with the same emergent spectrum on the transverse axis may have different well chamber calibration coefficients. X-ray spectrometry measurements performed by NIST have quantified such anisotropy by calculating the air-kerma rate from the emergent spectrum as a function of seed rotation angle in the plane of the seed axis (Mitch and Seltzer 2005). These measurements demonstrated that ^{125}I seeds containing silver spheres have a more anisotropic emission pattern than those containing silver wires. The well chamber calibration coefficients for the two ^{125}I silver sphere seed models have larger values than those for the six silver wire seed models, even though all eight models have the same emergent spectrum on the transverse axis (see figure 16-2). This is because the photons emergent from the ends of the silver sphere seeds are more attenuated than those from the ends of the silver wire seeds. Therefore, for ^{125}I seeds with silver wires, the 4π geometry of the well chamber results in more photons being detected by the well chamber that fall outside the beam acceptance cone of the WAFAC than in the case of the silver sphere seeds. This results in a larger well chamber ionization current for silver wire seeds relative to the WAFAC-measured air-kerma strength, and thus a lower value of the calibration coefficient (S_K/I) compared to that for silver sphere seeds. This observation also holds true for the one ^{103}Pd seed model that contains silver spheres, as shown in figure 16-2.

5.2.2 Beta Sources

The secondary standard calibration procedures for beta-particle seed and line sources using well-ionization chambers are very similar to those of the photon-emitting seeds described above. However, since beta sources are calibrated in terms of absorbed-dose-rate to water, the calibration coefficient, \dot{D}_w/I , is defined as the ratio of the dose-rate-to-water at a specified depth (2 mm for AAPM protocols) to the well chamber ionization current, typically expressed in units of Gy/A. Sometimes special designs of the seed centering insert are used to position the source more precisely at the “sweet spot” with a minimum of lateral uncertainty. Also, to enhance response to beta particles, thinner entrance walls for the ionization volume can be used.

5.3 Detectors for Absorbed-Dose Measurements

A number of detectors have been employed in the past for direct measurements of absorbed dose rate in water or water-equivalent plastic. All of these detectors are

described in detail in chapters 23 through 32, but a few which are especially suited for the demands of brachytherapy dosimetry are pointed out here. What makes the dosimetry of these sources so difficult are the very high dose-rate gradients near the sources. Gradients on the order of 100% per millimeter are typical, so a premium is placed on dosimeter thickness so as to minimize volume-averaging effects. In addition, because of the strong Z dependence of the photoelectron cross section below 100 keV, most detector materials exhibit a strong energy dependence of the detectors absorbed dose sensitivity in this energy region. Thus there is a premium placed on water-equivalent detector materials. These two requirements rule out many of the detection systems described in chapters 23 through 32, with the exception of thin thermoluminescent dosimeters, radiochromic film, gel dosimeters, and small volume scintillators, and even these detectors are difficult to use in brachytherapy applications.

References

- Baker, M., G. A. Bass, and M. J. Woods. (2002). "Calibration of the NPL secondary standard radionuclide calibrator for ^{125}I seeds used for prostate brachytherapy." *Appl Radiat Isot* 56:321–325.
- Bambynek, M. (2002). "Development of a multi-electrode extrapolation chamber as a prototype of a primary standard for the realization of the quantity of the absorbed dose to water for beta radiation brachytherapy sources." *Nucl Instrum Methods A* 492:264–275.
- Borg, J., I. Kawrakow, D. W. O. Rogers, and J. P. Seuntjens. (2000). "Monte Carlo study of correction factors for Spencer-Attix cavity theory at photon energies at or above 100 keV." *Med Phys* 27:1804–1813.
- Culberson, W. S., L. A. DeWerd, D. R. Anderson, and J. A. Micka. (2006). "Large-volume ionization chamber with variable apertures for air-kerma measurements of low-energy radiation sources." *Rev Sci Instrum* 77:015105–9.
- Das, R. K., V. Mishra, H. Perera, A. S. Meigooni, and J. F. Williamson. (1995). "A secondary air kerma strength standard for ^{169}Yb interstitial brachytherapy sources." *Phys Med Biol* 40:741–756.
- Douysset, G., J. Gouriou, F. Delaunay, L. DeWerd, K. Stump, and J. Micka. (2005). "Comparison of dosimetric standards of USA and France for HDR brachytherapy." *Phys Med Biol* 50:1961–1978.
- Goetsch, S. J., F. H. Attix, D. W. Pearson, and B. R. Thomadsen. (1991). "Calibration of ^{192}Ir high-dose-rate afterloading systems." *Med Phys* 18:462–467.
- Li, Z., R. K. Das, L. A. DeWerd, G. S. Ibbott, A. S. Meigooni, J. Pérez-Calatayud, M. J. Rivard, R. S. Sloboda, and J. F. Williamson. (2007). "Dosimetric prerequisites for routine clinical use of photon emitting brachytherapy sources with average energy higher than 50 keV." *Med Phys* 34:37–40.
- Loevinger, R., and N. G. Trott. (1966). "Design and operation of an extrapolation chamber with removable electrodes." *Int J Appl Radiat Isot* 17:103–111.
- Loftus, T. P. (1969). "Standardization of ^{137}Cs gamma-ray sources in terms of exposure units (Roentgens)." *J Res Natl Bur Stand* 74A:1–6.
- Loftus, T. P. (1979). "Standardization of ^{192}Ir gamma-ray sources in terms of exposure." *J Res Natl Bur Stand* 85:19–25.

- Mainegra-Hing, E., and D. W. O. Rogers. (2006). "On the accuracy of techniques for obtaining the calibration coefficient NK of ^{192}Ir HDR brachytherapy sources." *Med Phys* 33:3340–3346.
- Mitch, M. G., and S. M. Seltzer. (2005). "Using x-ray spectrometry to quantify the effects of emission anisotropy on air-kerma-strength measurements of prostate brachytherapy seeds." *Med Phys* 32:2129.
- Mitch, M. G., P. J. Lamperti, S. M. Seltzer, and B. M. Coursey. (2002). "New methods for anisotropy characterization of ^{103}Pd and ^{125}I prostate brachytherapy seed emissions using radiochromic film and angular x-ray spectrometry." *Med Phys* 29:1228.
- Monroe, J. I., and J. F. Williamson. (2002). "Monte-Carlo aided dosimetry of the Theragenics TheraSeed Model 200 ^{103}Pd interstitial brachytherapy seed." *Med Phys* 29:609–621.
- Rivard, M. J., B. M. Coursey, L. A. DeWerd, W. F. Hanson, M. S. Huq, G. S. Ibbott, M. G. Mitch, R. Nath, and J. F. Williamson. (2004). "Update of AAPM Task Group No. 43 Report: A revised AAPM protocol for brachytherapy dose calculations." *Med Phys* 31:633–674. Also available as AAPM Report No. 84.
- Rossiter, M. J., T. T. Williams, and G. A. Bass. (1991). "Air kerma rate calibration of small sources of ^{60}Co , ^{137}Cs , ^{226}Ra and ^{192}Ir ." *Phys Med Biol* 36:279–284.
- Sander, T., and R. F. Nutbrown. (2006). "The NPL air kerma primary standard TH100C for high dose rate ^{192}Ir brachytherapy sources." NPL Report DQL-RD 004 ISSN 1744-0637. <http://publications.npl.co.uk>.
- Sarfehnia, A., K. Stewart, and J. Seuntjens. (2007). "An absorbed dose to water standard for HDR ^{192}Ir brachytherapy sources based on water calorimetry: Numerical and experimental proof-of-principle." *Med Phys* 34:4957–4961.
- Selbach, H. J., H. M. Kramer, and W. S. Culbertson. (2008). "Realization of reference air-kerma rate for low-energy photon sources." *Metrologia* 45:422–428.
- Seltzer, S. M., and P. M. Bergstrom. (2003). "Changes in the U.S. primary standards for the air kerma from gamma-ray beams." *J Res Natl Inst Stand Technol* 108:359–381.
- Seltzer, S. M., P. J. Lamperti, R. Loevinger, M. G. Mitch, J. T. Weaver, and B. M. Coursey. (2003). "New national air-kerma-strength standards for ^{125}I and ^{103}Pd brachytherapy seeds." *J Res Natl Inst Stand Technol* 108:337–358.
- Sephton, J. P., M. J. Woods, M. J. Rossiter, T. T. Williams, J. C. Dean, G. A. Bass, and S. E. Lucas. (1993). "Calibration of the NPL secondary standard radionuclide calibrator for ^{192}Ir brachytherapy sources." *Phys Med Biol* 38:1157–1164.
- Soares, C. G. (1991). "Calibration of ophthalmic applicators at NIST—a revised approach." *Med Phys* 18:787–793.
- Soares, C. G., D. G. Halpern, and C. K. Wang. (1998). "Calibration and characterization of beta-particle sources for intravascular brachytherapy." *Med Phys* 25:339–346.
- Soares, C. G., G. Douysset, and M. G. Mitch. (2009). "Primary standards and dosimetry protocols for brachytherapy sources." CCRI special issue in *Metrologia*, In press.
- Taylor, R. E. P., and D. W. O. Rogers. (2008). "More accurate fitting of ^{125}I and ^{103}Pd radial dose functions." *Med Phys* 35:4242–4250.
- VanDamme, J. J., W. S. Culbertson, L. A. DeWerd, and J. A. Micka. (2008). "Air-kerma strength determination of a ^{169}Yb high dose rate brachytherapy source." *Med Phys* 35:3935–3942.
- van Dijk, E., I. K. Kolkman-Deurloo, and P. M. G. Damen. (2004). "Determination of the reference air kerma rate for ^{192}Ir brachytherapy sources and the related uncertainty." *Med Phys* 31:2826–2833.

Problems

1. A WAFAC measurement of the strength of an ^{125}I brachytherapy seed yields the following currents, decay corrected to a reference date and time of January 12, 2009 at 00:00:01 EST: $I_1 = 2.08 \times 10^{-13}$ A for a chamber volume of 804 cm^3 , $I_2 = 5.31 \times 10^{-14}$ A for a chamber volume of 216 cm^3 . Find the air-kerma strength of the seed at the reference date and time given above in units of $\mu\text{Gy m}^2/\text{h}$, assuming that $\frac{\bar{W}}{e} = 33.97 \text{ J / C}$, $\rho_{air} = 1.18 \text{ mg / cm}^3$, $K_{dr}(\dot{K}) = 1.0001$, and $d = 30 \text{ cm}$.
2. A nominal $100 \text{ mCi } ^{90}\text{Sr}/^{90}\text{Y}$ ophthalmic applicator gives rise to an absorbed dose rate to water of about 0.5 Gy/s on the surface of the applicator. This dose rate in turn yields a 200 pA/mm limiting value of the slope in the extrapolation chamber curve using the 4 mm diameter collecting electrode. If the system noise levels are such that the lower level of measurement is about 1 pA/mm , what is the minimum measurable dose rate with the system when using the 1 mm diameter collecting electrode?

